J. Am. Chem. Soc. **1981**, *103*, 1932–1941

Structural Characterization of the $[Fe_4(S_2C_2(CF_3)_2)_4(\mu_3\text{-}S)_4]^{2-}$ Dianion. Stereochemical Relationship between the Cubanelike Fe_4S_4 Cores of This Balch Dithiolene Dianion and the $[Fe_4(\eta^5\text{-}C_5H_5)_4(\mu_3\text{-}S)_4]^{2+}$ Dication and Resulting Electronic Implications

Timothy H. Lemmen, Joseph A. Kocal, Frederick Yip-Kwai Lo, Michael W. Chen, and Lawrence F. Dahl*

Contribution from the Department of Chemistry, University of Wisconsin—Madison, Madison, Wisconsin 53706. Received June 2, 1980

Abstract: An X-ray crystallographic analysis of the tetrakis(*cis*-1,2-bis(trifluoromethyl)ethylene-1,2-dithiolato)tetrairon tetrasulfide dianion as the tetraphenylarsonium salt has provided (1) unequivocal proof that its central cubanelike Fe_4S_4 core experimentally conforms to a regular tetragonal D_{2d}—$\bar{4}2m$ geometry whose Fe–Fe and Fe–S dimensions closely resemble those of the Fe_4S_4 core in the $[Fe_4(\eta^5\text{-}C_5H_5)_4(\mu_3\text{-}S)_4]^{2+}$ dication and (2) the correct coordination (previously assumed to be a distorted trigonal-bipyramidal arrangement) of five sulfur atoms about each chemically equivalent iron atom. The Fe_4S_4 framework of the dianion possesses a uniformly compressed iron tetrahedron (along the S_4—$\bar{4}$ axis) with four shorter lengths of mean 2.855 Å and two longer lengths of mean 3.442 Å; the four vertical Fe–S bonds (approximately parallel to the S_4 axis) of mean 2.153 Å are 0.09 Å shorter than the other eight equivalent Fe–S bonds of mean 2.247 Å. The disposition of the four $S_2C_2(CF_3)_2$ ligands about the Fe_4S_4 core gives rise to a nearly regular square-pyramidal sulfur environment about each iron atom. Inclusion of the dithiolene ligands results in a small but significant sterically induced angular distortion which lowers the symmetry for the entire dianion to an approximate S_4 configuration. A geometrical comparison of the four equivalent (Fe–Fe)-bonded Fe_2S_2 fragments in the dianion is made with the planar Fe_2S_2 fragment possessed by the $[Fe_2(S_2C_2(CF_3)_2)_4]^-$ monoanion and other $[M_2(S_2X)_4]^n$ dimers (M = Fe, Co), and the resulting bonding implications are discussed. The geometrically similar Fe_4S_4 cores in the $[Fe_4(S_2C_2(CF_3)_2)_4(\mu_3\text{-}S)_4]^{2-}$ dianion and $[Fe_4(\eta^5\text{-}C_5H_5)_4(\mu_3\text{-}S)_4]^{2+}$ dication provide evidence for equivalent Fe–Fe interactions and thereby furnish a basis for the application of a qualitative metal cluster model which not only correlates the electronic configuration of the dianion with its geometry but also enables a prediction of probable geometrical changes expected for the other two isolated members ($n = 0, -1$) of the $[Fe_4(S_2C_2(CF_3)_2)_4(\mu_3\text{-}S)_4]^n$ series. $[AsPh_4]_2{}^+[Fe_4(S_2C_2(CF_3)_2)_4(\mu_3\text{-}S)_4]^{2-}$ crystallizes in a monoclinic unit cell of $P2_1/n$ symmetry with lattice constants $a = 13.832$ (3) Å, $b = 37.279$ (7) Å, $c = 14.973$ (3) Å, $\beta = 101.27$ (4)°, and $V = 7572.0$ Å^3; $\rho_{calcd} = 1.78$ g/cm^3 for $Z = 4$. Least-squares refinement (with anisotropic thermal coefficients for the As, Fe, and S atoms, isotropic temperature factors for the C and F atoms, and a rigid-group constraint for each of the eight phenyl rings) gave $R_1(F) = 12.6\%$ and $R_2(F) = 11.7\%$ for 3899 independent diffractometry collected data with $I > 2\sigma(I)$.

The work presented herein is an outgrowth of our structural investigations of the $[Fe_4(\eta^5\text{-}C_5H_5)_4(\mu_3\text{-}S)_4]^n$ clusters ($n = 0$,[1] 1,[2] 2[3]) for the purpose of establishing a correlation between geometry and electronic configuration in this cubanelike Fe_4S_4 series. A crystallographic analysis of the dication revealed an unanticipated tetragonal D_{2d} geometry for its Fe_4S_4 core with four relatively short and two long Fe–Fe distances. Of particular interest is the overall resemblance of this architecture with that of the bis(trifluoromethyl)-1,2-dithiolene dianion of the $[Fe_4L_4(\mu_3\text{-}S)_4]^n$ series (L = $S_2C_2(CF_3)_2$, $n = 0, -1, -2$) whose members were synthesized, isolated, and physicochemically characterized by Balch.[4] An X-ray diffraction examination of $[NBu_4]_2{}^+[Fe_4(S_2C_2(CF_3)_2)_4(\mu_3\text{-}S)_4]^{2-}$ was carried out by Bernal and Davis,[5a] who were unable to refine the crystal structure due to a crystallographic disorder problem which involved the nonresolution of the two independent tetra-*n*-butylammonium cations. Although the large observed variations in the Fe–Fe, Fe–S, and S···S distances of the Fe_4S_4 framework (e.g., the six reported Fe–Fe distances are 2.58, 2.75, 2.78, 2.80, 3.19, and 3.26 Å with esd's of 0.02 Å) prevented an assignment[5] of any idealized geometry to this cluster, we subsequently concluded[3] that under assumed D_{2d} symmetry the resulting mean distances and mean bond angles corresponded in a gross fashion to those of the $[Fe(\eta^5\text{-}C_5H_5)_4(\mu_3\text{-}S)_4]^{2+}$ dication. We, therefore, proposed[3] that the idealized Fe_4S_4 architecture in the iron dithiolene anion is structurally and electronically similar to that in the iron cyclopentadienyl dication. In order to provide an operational test of this hypothesis, it was necessary to perform an X-ray diffraction study on the tetraphenylarsonium salt of the $[Fe_4(S_2C_2(CF_3)_2)_4(\mu_3\text{-}S)_4]^{2-}$ dianion which was prepared and isolated via the Balch procedure.[4] The results given here are relevant not only in connection with the Mössbauer data reported by Good and Chandra[5a] and later by Reiff and co-workers[5b] for the $[Fe_4(S_2C_2(CF_3)_2)_4(\mu_3\text{-}S)_4]^n$ tetramers ($n = 0, -1, -2$ as the $[AsPh_4]^+$ salts) but also with respect to the remarkably different structural-bonding influences found when other terminal ligands such as SR,[6] Cl,[7] NO,[8] and (CO)$_3$[9] are coordinated with each iron atom of an Fe_4S_4 core. The fact that the $[Fe_4(SR)_4(\mu_3\text{-}S)_4]^n$ series ($n = -1, -2, -3$) has been shown from extensive studies of their structural and physicochemical properties by Holm, Ibers, and co-workers[10] to be the first well-defined synthetic analogues of

---

[1] (a) Wei, C. H.; Wilkes, G. R.; Treichel, P. M.; Dahl, L. F. *Inorg. Chem.* **1966**, *5*, 900–905. (b) Schunn, R. A.; Fritchie, C. J., Jr.; Prewitt, C. T. *Ibid.* **1966**, *5*, 892–899.

[2] Trinh-Toan; Fehlhammer, W. P.; Dahl, L. F. *J. Am. Chem. Soc.* **1977**, *99*, 402–407.

[3] Trinh-Toan; Teo, B. K.; Ferguson, J. A.; Meyer, T. J.; Dahl, L. F. *J. Am. Chem. Soc.* **1977**, *99*, 408–416.

[4] Balch, A. L. *J. Am. Chem. Soc.* **1969**, *91*, 6962–6967.

[5] (a) Bernal, I.; Davis, B. R.; Good, M. L.; Chandra, S. *J. Coord. Chem.* **1972**, *2*, 61–65. (b) Frankel, R. B.; Reiff, W. M.; Bernal, I.; Good, M. L. *Inorg. Chem.* **1974**, *13*, 493–494.

[6] (a) Laskowski, E. J.; Reynolds, J. G.; Frankel, R. G.; Foner, S.; Papaefthymiou, G. C.; Holm, R. H. *J. Am. Chem. Soc.* **1979**, *101*, 6562–6570 and references cited therein. (b) Berg, J. M.; Hodgson, K. O.; Holm, R. H. *Ibid.* **1979**, *101*, 4586–4593 and references cited therein.

[7] Bobrik, M. A.; Hodgson, K. O.; Holm, R. H. *Inorg. Chem.* **1977**, *16*, 1851–1858.

[8] (a) Gall, R. S.; Chu, C. T.-W.; Dahl, L. F. *J. Am. Chem. Soc.* **1974**, *96*, 4019–4023. (b) Chu, C. T.-W.; Lo, F. Y.-K.; Dahl, L. F., submitted for publication.

[9] Nelson, L. L.; Lo, F. Y.-K.; Rae, A. D.; Dahl, L. F., unpublished research.

0002-7863/81/1503-1932$01.25/0

the Fe_4S_4 cluster units in bacterial ferredoxins and in the high-potential iron proteins has stimulated considerable interest concerning structural differences in these Fe_4S_4 complexes.

Experimental Section

Crystal Data. $[AsPh_4]_2{}^+[Fe_4(S_2C_2(CF_3)_2)_4(\mu_3\text{-}S)_4]^{2-}$ (fw = 2023.0) was synthesized and black crystals were obtained as described previously.[4] A suitable parallelepiped-shaped crystal of dimensions 0.40 × 0.28 × 0.25 mm was mounted and sealed in a glass capillary under an argon atmosphere. Intensity data were obtained with Mo Kα radiation on a Syntex $P\bar{1}$ diffractometer via the ω scan method. The detailed procedures of crystal alignment, data collection, and treatment of the diffraction data are given elsewhere.[11] An analytical absorption correction[12] was applied to the intensity data in that the calculated transmission coefficients (based upon a calculated linear absorption coefficient of 21.1 cm^{-1} for Mo Kα radiation) ranged from 0.52 to 0.68. Lattice constants measured at ca. 22 °C for the chosen monoclinic unit cell are a = 13.832 (3) Å, b = 37.279 (7) Å, c = 14.973 (3) Å, and β = 101.27 (4)°; the unit cell volume of 7572.0 Å^3 gives rise to a calculated density of 1.775 g/cm^3 for Z = 4.

Structural Determination and Refinement. Systematic absences of $\{h0l\}$ for $h + l$ odd and $\{0k0\}$ for k odd uniquely define the probable space group to be $P2_1/n$. The crystallographically independent unit consists of two tetraphenylarsonium cations and one dianion; this corresponds to 2 arsenic, 4 iron, 12 sulfur, 24 fluorine, and 64 carbon atoms each occupying the fourfold set of general positions $\pm(x, y, z; {}^1/_2 + x, {}^1/_2 - y, {}^1/_2 + z)$.

A three-dimensional Patterson map[13] provided initial coordinates for the two arsenic and four iron atoms. Successive Fourier and difference Fourier syntheses[13] eventually yielded coordinates for all 106 nonhydrogen atoms. Least-squares refinement[14-17] was performed with anisotropic thermal parameters utilized for the arsenic, iron, and sulfur atoms and isotropic temperature factors for the carbon and fluorine atoms. Each of the eight phenyl rings was constrained to its well-known geometry and refined as a rigid group. The final refinement converged at $R_1(F)$ = 12.6% and $R_2(F)$ = 11.7%[15] for 3899 independent reflections with $I > 2\sigma(I)$; the "goodness-of-fit" value[15] was 1.70, while all shift-over-error ratios were less than 1.2. A final difference Fourier map revealed no anomalous features. The relatively high discrepancy factors are attributed mainly to the composite effects of residual overlap of adjacent diffraction maxima (due to the long b axial length) and presumed anisotropic thermal behavior of the dithiolene carbon and fluorine atoms as evidenced by their large isotropic temperature factors. Our arbitrary use of an isotropic thermal model for all carbon and fluorine atoms was based upon program-size limitations (at the time of the refinement) coupled with a reluctance to lower the data-to-parameter ratio[15] of 9.3/1. Our satisfaction with the refined crystal structure stems from our primary interest in the structural features of the Fe_4S_4 core, for which the corresponding distances and bond angles are equivalent within experimental error under assumed tetragonal D_{2d} symmetry.

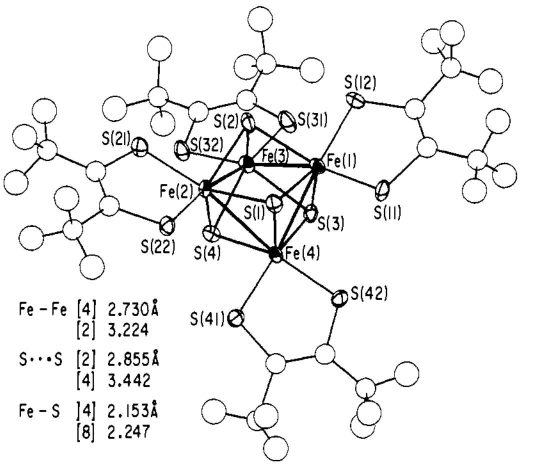

Figure 1. $[Fe_4(S_2C_2(CF_3)_2)_4(\mu_3\text{-}S)_4]^{2-}$ dianion of idealized tetragonal S_4—$\bar{4}$ configuration. Its Fe_4S_4 core experimentally conforms to D_{2d}—$\bar{4}2m$ symmetry.

The positional and thermal parameters from the output of the final full-matrix least-squares cycle are given in Table I. Interatomic distances and bond angles[18] are presented in Table II, while selected least-squares planes and interplanar angles[19] are given in Table III. Observed and calculated structure factors are listed as supplementary material. All molecular configurations were computer generated and computer drawn.[20]

Results and Discussion

General Description of the Crystal Structure. The solid-state structure of $[AsPh_4]_2{}^+[Fe_4(S_2C_2(CF_3)_2)_4(\mu_3\text{-}S)_4]^{2-}$ is expectedly composed of discrete monocations and dianions. There is no evidence of unusual interionic interactions in that the shortest interionic F···C(phenyl) contacts are ca. 3.1 Å (possibly involving weak F···H–C bonding).

Figure 1 displays the configuration of the $[Fe_4(S_2C_2(CF_3)_2)_4(\mu_3\text{-}S)_4]^{2-}$ dianion which possesses within experimental error a cubanelike Fe_4S_4 core of tetragonal D_{2d} symmetry that is reduced to S_4 symmetry by inclusion of the dithiolene ligands (vide infra). Although the overall architecture is similar in a gross fashion to that of the $[Fe_4(S_2)_4(\mu_3\text{-}S)_4]^{2-}$ fragment illustrated in a figure by Bernal and Davis[5a] for the partially solved (uncooperative) crystal structure of the $[NBu_4]^+$ salt, the large apparent uncertainties in the positional parameters of the iron and sulfur atoms in this latter structure preclude any physically meaningful comparison between the two structures. The two independent tetraphenylarsonium cations each possess normal As–C distances with identical means of 1.89 Å and expected variations of the six tetrahedral C–As–C bond angles within 107.5–111.0° and 106.4–113.4° ranges.

The $[Fe_4(S_2C_2(CF_3)_2)_4(\mu_3\text{-}S)_4]^{2-}$ Dianion. (a) Previously Determined Physicochemical Properties. The air-stable $[Fe_4(S_2C_2(CF_3)_2)_4(\mu_3\text{-}S)_4]^{2-}$ dianion was first reported in 1969 by Balch[4] who prepared the tetraphenylarsonium and tetrabutylammonium salts of the dianion by reduction of the neutral parent; this reduction was achieved by dissolution of the neutral parent in dimethyl sulfoxide as a basic solvent. In turn, the neutral parent was synthesized[4] by the reaction of $Fe_2(CO)_6(S_2C_2(CF_3)_2)$ and sulfur in refluxing xylene. Polarographic measurements of this dianion in dichloromethane solution revealed two anodic and two cathodic waves at nearly the same voltages as those obtained from a polarographic examination of the neutral parent which exhibited four successive cathodic waves. This electrochemical indication for the existence of a corresponding tetrameric monoanion led to its isolation by Balch[4] from the reaction of the neutral parent with $[AsPh_4]_2{}^+[Fe_4(S_2C_2(CF_3)_2)_4(\mu_3\text{-}S)_4]^{2-}$. Because of their presumed

---

(10) Ibers, J. A.; Holm, R. H. *Science (Washington, D.C.)* **1980**, *209*, 223–235 and references cited therein.

(11) Byers, L. R.; Dahl, L. F. *Inorg. Chem.* **1980**, *19*, 680–692 and references cited therein.

(12) Blount, J. F. "DEAR, A Local FORTRAN Absorption-Correction Program", 1965, based on the method given by: Busing, W. R.; Levy, H. A. *Acta Crystallogr.* **1957**, *10*, 180–182.

(13) Calabrese, J. C. "MAP, A FORTRAN Fourier Summation and Molecular Assemblage Program"; University of Wisconsin-Madison: Madison, WI, 1972.

(14) "ORFLSR, A Local Rigid-Body Least-Squares Program" (adapted from the Busing–Martin–Levy ORFLS); Report ORNL-TM-305; Oak Ridge National Laboratory, Oak Ridge, TN, 1963.

(15) The unweighted and weighted discrepancy factors used are $R_1(F) = [\sum||F_o| - |F_c||/\sum|F_o|] \times 100$ and $R_2(F) = [\sum w_i||F_o| - |F_c||^2/\sum w_i|F_o|^2]^{1/2} \times 100$. All least-squares refinements were based on the minimization of $\sum w_i||F_o| - |F_c||^2$ with individual weights of $w_i = 1/\sigma^2(F_o)$ assigned on the basis of the esd's of the observed structure factors. The standard deviation in an observation of unit weight ("goodness-of-fit") is defined by $[\sum w_i(|F_o| - |F_c|)^2/(m - n)]^{1/2}$, where the number of reflections (m) was 3899 and the number of parameters varied in the refinement (n) was 419, from which $m/n = 9.3/1$.

(16) Atomic scattering factors for neutral atoms were used.[17a,b] Anomalous dispersion corrections[17c] were applied to the scattering factors of the As, Fe, and S atoms.

(17) (a) Cromer, D. T.; Mann, J. B. *Acta Crystallogr., Sect. A* **1968**, *A24*, 321–324. (b) Stewart, R. F.; Davidson, E. R.; Simpson, W. T. *J. Chem. Phys.* **1965**, *42*, 3175–3187. (c) Reference 12, p 149.

(18) Busing, W. R.; Martin, K. O.; Levy, H. A. "ORFFE, A FORTRAN Crystallographic Function and Error Program"; Report ORNL-TM-306; Oak Ridge National Laboratory: Oak Ridge, TN, 1964.

(19) "PLANES". A revised version of "PLANE 1" written by: Smith, D. L. Ph.D. Thesis, University of Wisconsin-Madison, 1962; Appendix IV.

(20) Johnson, C. K. "ORTEP-II, A FORTRAN Thermal-Ellipsoid Plot Porgram for Crystal Structure Illustrations"; Report ORNL-5138; Oak Ridge National Laboratory: Oak Ridge, TN, 1976.

Table I. Atomic Parameters for $[AsPh_4]_2^+[Fe_4(S_2C_2(CF_3)_2)_4(\mu_3\text{-}S)_4]^{2-}$

A. Positional and Isotropic Temperature Factors (Å^2)^{a,b}

atom	10^4x	10^4y	10^4z	B, Å^2	atom	10^4x	10^4y	10^4z	B, Å^2
Fe(1)	6457 (3)	4166 (1)	7146 (3)	*b*	F(22)	3294 (20)	3350 (7)	9865 (17)	8.1 (7)
Fe(2)	5091 (3)	3810 (1)	5376 (3)	*b*	F(23)	4748 (23)	3444 (8)	10296 (21)	10.8 (10)
Fe(3)	7036 (3)	3660 (1)	6042 (3)	*b*	F(24)	4304 (21)	2939 (9)	9987 (19)	9.8 (9)
Fe(4)	5263 (3)	3588 (1)	7143 (3)	*b*	As(1)	10142 (3)	7127 (1)	10104 (3)	*b*
S(1)	4830 (6)	4112 (3)	6607 (6)	*b*	As(2)	7234 (3)	4857 (1)	3029 (3)	*b*
S(2)	6409 (6)	4177 (3)	5631 (6)	*b*	C(1-1)	10012	6618	10103	2.5 (7)
S(3)	6906 (6)	3624 (3)	7510 (6)	*b*	C(1-2)	9224	6444	9555	2.9 (8)
S(4)	5698 (6)	3310 (2)	5951 (6)	*b*	C(1-3)	9142	6073	9594	3.9 (8)
S(11)	6099 (7)	4396 (3)	8382 (6)	*b*	C(1-4)	9848	5876	10181	4.3 (9)
S(12)	7714 (7)	4516 (3)	7307 (7)	*b*	C(1-5)	10636	6050	10729	4.8 (10)
S(21)	5228 (6)	3777 (3)	3955 (6)	*b*	C(1-6)	10718	6421	10690	4.7 (9)
S(22)	3501 (6)	3779 (3)	4928 (6)	*b*	C(2-1)	9292	7316	9103	3.5 (8)
S(31)	8619 (7)	3748 (3)	6491 (7)	*b*	C(2-2)	9615	7392	8301	4.6 (10)
S(32)	7354 (6)	3350 (3)	4900 (6)	*b*	C(2-3)	8951	7515	7543	6.8 (12)
S(41)	3931 (7)	3261 (3)	6925 (7)	*b*	C(2-4)	7964	7560	7587	4.9 (10)
S(42)	5295 (7)	3547 (3)	8583 (6)	*b*	C(2-5)	7641	7484	8389	6.9 (11)
C(11)	7045 (25)	4698 (9)	8816 (24)	3.0 (8)	C(2-6)	8305	7361	9147	3.8 (9)
C(12)	7761 (23)	4735 (9)	8355 (21)	2.4 (7)	C(3-1)	11454	7254	9995	2.7 (7)
C(13)	6980 (48)	4873 (18)	9742 (42)	9.6 (17)	C(3-2)	11720	7613	10122	2.8 (7)
C(14)	8646 (41)	4977 (16)	8695 (39)	8.1 (15)	C(3-3)	12657	7724	10038	5.4 (10)
C(21)	4038 (24)	3706 (9)	3346 (23)	2.9 (8)	C(3-4)	13328	7476	9825	6.4 (12)
C(22)	3316 (23)	3701 (8)	3788 (21)	2.3 (7)	C(3-5)	13062	7117	9698	5.9 (11)
C(23)	4031 (33)	3633 (12)	2373 (29)	5.0 (10)	C(3-6)	12125	7006	9782	5.1 (10)
C(24)	2180 (29)	3659 (12)	3292 (27)	4.1 (9)	C(4-1)	9883	7326	11189	3.0 (8)
C(31)	9173 (26)	3553 (9)	5702 (23)	3.0 (8)	C(4-2)	9492	7670	11159	3.6 (8)
C(32)	8630 (22)	3379 (9)	4962 (21)	2.1 (7)	C(4-3)	9344	7834	11955	4.7 (9)
C(33)	10320 (46)	3608 (19)	5844 (44)	10.0 (18)	C(4-4)	9587	7654	12781	4.3 (10)
C(34)	9013 (36)	3186 (14)	4234 (34)	6.5 (12)	C(4-5)	9978	7310	12811	3.9 (9)
C(41)	3678 (20)	3177 (8)	7945 (20)	1.6 (7)	C(4-6)	10126	7146	12015	3.2 (8)
C(42)	4268 (25)	3326 (9)	8721 (24)	3.0 (8)	C(5-1)	7975	4949	4207	3.8 (8)
C(43)	2730 (52)	2898 (18)	8053 (42)	13.3 (18)	C(5-2)	8511	4679	4722	2.9 (7)
C(44)	4182 (44)	3284 (17)	9668 (41)	8.8 (16)	C(5-3)	9020	4751	5599	3.1 (8)
F(1)	6116 (23)	4851 (8)	9882 (20)	10.0 (9)	C(5-4)	8995	5093	5961	4.2 (9)
F(2)	7274 (23)	5201 (9)	9767 (21)	11.2 (10)	C(5-5)	8459	5363	5446	6.4 (12)
F(3)	7544 (26)	4718 (9)	10391 (23)	12.4 (11)	C(5-6)	7950	5291	4569	4.6 (9)
F(4)	8513 (20)	5305 (8)	8385 (18)	8.6 (8)	C(6-1)	7361	5272	2318	3.4 (8)
F(5)	9021 (20)	4973 (8)	9494 (20)	9.0 (8)	C(6-2)	6572	5443	1765	3.4 (9)
F(6)	9411 (20)	4891 (7)	8250 (18)	8.9 (8)	C(6-3)	6729	5751	1291	5.0 (10)
F(7)	3776 (17)	3287 (7)	2111 (16)	7.2 (7)	C(6-4)	7677	5888	1370	4.6 (10)
F(8)	3302 (16)	3833 (6)	1801 (15)	5.7 (6)	C(6-5)	8466	5717	1923	8.5 (14)
F(9)	4808 (18)	3708 (6)	2052 (16)	7.0 (6)	C(6-6)	8309	5409	2397	5.7 (11)
F(10)	2060 (18)	3415 (7)	2679 (17)	7.9 (7)	C(7-1)	5892	4774	3030	4.7 (9)
F(11)	1847 (18)	3975 (7)	2871 (17)	7.7 (7)	C(7-2)	5551	4830	3833	6.9 (12)
F(12)	1624 (16)	3613 (7)	3888 (15)	5.7 (6)	C(7-3)	4565	4771	3859	6.3 (11)
F(13)	10781 (19)	3353 (7)	5564 (17)	7.7 (7)	C(7-4)	3920	4654	3082	6.0 (11)
F(14)	10494 (22)	3884 (9)	5344 (21)	10.8 (9)	C(7-5)	4261	4598	2279	4.8 (10)
F(15)	10673 (22)	3689 (8)	6668 (21)	10.2 (9)	C(7-6)	5247	4657	2254	5.3 (11)
F(16)	8293 (18)	3078 (6)	3528 (16)	6.9 (7)	C(8-1)	7762	4438	2599	5.8 (12)
F(17)	9677 (19)	3372 (7)	3870 (17)	7.6 (7)	C(8-2)	7319	4105	2633	8.3 (14)
F(18)	9448 (19)	2868 (8)	4574 (17)	8.8 (8)	C(8-3)	7754	3800	2350	11.5 (18)
F(19)	2774 (20)	2753 (8)	8647 (20)	12.8 (8)	C(8-4)	8630	3828	2033	8.9 (17)
F(20)	2038 (21)	3182 (8)	8066 (19)	13.3 (9)	C(8-5)	9073	4161	1999	7.2 (13)
F(21)	2388 (20)	2845 (8)	7241 (19)	12.0 (8)	C(8-6)	8638	4466	2282	5.8 (11)

B. Anisotropic Thermal Parameters (× 10^4)^{a,b}

atom	β_{11}	β_{22}	β_{33}	β_{12}	β_{13}	β_{23}	atom	β_{11}	β_{22}	β_{33}	β_{12}	β_{13}	β_{23}
Fe(1)	24 (3)	5 (0)	32 (3)	−2 (1)	0 (2)	−1 (1)	S(12)	38 (7)	6 (1)	47 (7)	−5 (2)	8 (5)	−1 (2)
Fe(2)	29 (3)	5 (0)	19 (3)	1 (1)	3 (2)	−3 (1)	S(21)	23 (6)	7 (1)	38 (6)	0 (2)	3 (5)	−2 (2)
Fe(3)	17 (3)	6 (1)	32 (3)	0 (1)	2 (3)	−1 (1)	S(22)	30 (6)	9 (1)	27 (6)	−3 (2)	−3 (4)	0 (2)
Fe(4)	27 (3)	5 (1)	27 (3)	−3 (1)	−4 (2)	0 (1)	S(31)	34 (7)	8 (1)	53 (7)	−6 (2)	6 (5)	−7 (2)
S(1)	29 (6)	6 (1)	37 (6)	−2 (2)	8 (5)	−4 (2)	S(32)	26 (6)	7 (1)	40 (6)	−2 (2)	3 (5)	−5 (2)
S(2)	40 (6)	6 (1)	31 (6)	−2 (2)	−7 (5)	−3 (2)	S(41)	41 (7)	10 (1)	30 (6)	−8 (2)	4 (5)	1 (2)
S(3)	38 (6)	4 (1)	21 (5)	2 (2)	−4 (4)	1 (2)	S(42)	40 (7)	9 (1)	29 (5)	−6 (2)	15 (5)	−2 (2)
S(4)	31 (6)	3 (1)	40 (6)	2 (2)	15 (5)	−2 (2)	As(1)	29 (3)	5 (0)	31 (2)	−1 (1)	−7 (2)	4 (1)
S(11)	56 (7)	7 (1)	23 (5)	0 (2)	10 (5)	−4 (2)	As(2)	47 (3)	8 (0)	47 (3)	2 (1)	3 (2)	4 (1)

C. Rigid-Body Parameters for the Eight Phenyl Rings^c

group	10^4x_b	10^4y_b	10^4z_b	μ, deg	σ, deg	ρ, deg	group	10^4x_b	10^4y_b	10^4z_b	μ, deg	σ, deg	ρ, deg
C_6H_5(1)	70	3753	−142	87.1	136.2	176.7	C_6H_5(5)	8485	5021	5084	17.7	174.6	−111.5
C_6H_5(2)	1372	2562	1655	−86.8	149.0	−110.8	C_6H_5(6)	7519	5580	1844	−93.3	−157.3	32.9
C_6H_5(3)	−2391	2635	90	16.3	−168.0	−5.3	C_6H_5(7)	4906	4714	3056	−176.4	105.6	185.8
C_6H_5(4)	265	2510	−1985	17.7	148.5	99.5	C_6H_5(8)	8196	4133	2316	−55.0	167.6	162.2

Footnotes to Table I

[a] In this and the following tables, estimated standard deviations are given in parentheses. [b] Anisotropic thermal parameters of the form $\exp[-(h^2\beta_{11} + k^2\beta_{22} + l^2\beta_{33} + 2hk\beta_{12} + 2hl\beta_{13} + 2kl\beta_{23})]$ were used for the Fe, S, and As atoms. [c] Each of the eight rings in the two independent tetraphenylarsonium cations was refined as a rigid group with hydrogens excluded. The six carbon atoms, C(*n*-*m*) (where *m* = 1–6), in a given phenyl ring *n* (where *n* = 1–8) were assigned individual isotropic temperature factors which were varied during the refinement. Each ring was assumed to have D_{6h} symmetry with C–C bond lengths of 1.39 Å. The internal orthogonal axial system x', y', z', for each phenyl ring *n* was defined as follows: the origin x_b, y_b, z_b was placed at the center of the carbon framework; x' was chosen along C(*n*-1)–C(*n*-4), y' along the perpendicular bisectors of C(*n*-2)–C(*n*-3) and C(*n*-5)–C(*n*-6), and z' along $x'xy'$. The three angles θ, ϕ, and ρ refer to the orientation of the internal axial system with respect to an external orthogonal system by rotations about y', x', and z', respectively. The orthogonal axes are defined in our program relative to the crystal axes as: $a_o = a$, $b_o = c_o \times a_o$, $c_o = a \times b$.

oxygen sensitivity, no effort was made by Balch[4] to isolate the $n = -3$ and $n = -4$ members of this electron-transfer series.

The formulation by Balch[4] of the dianion as a tetramer in preference to an alternate dimeric formulation, $[Fe_2(S_2C_2(CF_3)_2)_2S_2]^-$, was based upon (1) a conductivity study of the $[NBu_4]^+$ salt indicating that it behaves as a 2:1 electrolyte in acetonitrile solution and (2) magnetic susceptibility measurements which established the $[NBu_4]^+$ salt to be diamagnetic (instead of paramagnetic which would be required for a dimeric formulation) in acetone solution as well as in the solid state. Balch[4] also showed this tetrameric formulation for the dianion to be consistent with the corresponding tetrabutylammonium salt of the $[Fe_4(S_2C_2(CF_3)_2)_4S_4]^-$ monoanion being paramagnetic.

Because of their much lower solubilities, similar but less extensive studies were made by Balch[4] on the corresponding phenyl-substituted $[Fe_4(S_2C_2Ph_2)_4S_4]^n$ series ($n = 0, -1$). Evidence for its tetrameric nature was provided by isolating $[AsPh_4]^+$-$[Fe_4(S_2C_2Ph_2)_4S_4]^-$, shown from magnetic susceptibility and ESR measurements to be paramagnetic. In addition, polarographic measurements of both the neutral parent and monoanion indicated the monoanion to be the first reduced member of this electron-transfer series. It is especially noteworthy that the phenyl-substituted neutral parent of this series was originally reported in 1966 by Schrauzer and co-workers,[21] who prepared this sulfur-rich iron dithiolene complex from (1) the thermal degradation of $Fe(S_2C_2Ph_2)_2$, (2) the reaction of metallic iron or iron carbonyls with sulfur and diphenylacetylene, and (3) the reaction of $Fe_2(CO)_6(S_2C_2Ph_2)$ with sulfur. Their incorrect formulation of this neutral compound as a dimer, $Fe_2(S_2C_2Ph_2)_2S_2$, was apparently made on a chemically intuitive basis.

Balch[4] noted the considerable chemical stability of the iron–sulfur framework in $[Fe_4(S_2C_2(CF_3)_2)_4S_4]^n$ ($n = 0, -2$) and in $Fe_4(S_2C_2Ph_2)_4S_4$, as evidenced by these tetramers being unlike the bis(dithiolene) iron dimers in that they are not cleaved by triphenylarsine and triphenylstibine, even though these bases do reduce the neutral CF_3-substituted parent (but not the Ph-substituted analogue) to the monoanion. On the other hand, triphenylphosphine was found[4] to rupture the iron–sulfur bonds (by formation of triphenylphosphine sulfide) with the production of $Fe(S_2C_2R_2)_2PPh_3$ from the neutral complexes and of $[Fe_2(S_2C_2(CF_3)_2)_4]^{2-}$ from the dianion. The presence of "acid labile" sulfur in the $[Fe_4(S_2C_2(CF_3)_2)_4S_4]^{2-}$ dianion was also demonstrated[4] by its reactions with acid and mercuric ion.

On the basis of the above data, Balch[4] suggested two reasonable atomic arrangements for the members of these two series—one involving a cubanelike Fe_4S_4 framework and the other involving bridging by dithiolene ligands as well as by the "free" sulfur atoms. The former model was ascertained from the previously mentioned crystallographic study reported in 1972 by Bernal and Davis[5a] on the $[Fe_4(S_2C_2(CF_3)_2)_4(\mu_3\text{-}S)_4]^{2-}$ dianion as the $[NBu_4]^+$ salt. Although the overall configuration of the $[Fe_4(S_2)_4(\mu_3\text{-}S)_4]^{2-}$ fragment was established, its detailed structural features were not resolved because of a presumed crystal disorder of the counterions. At the same time, Good and Chandra[5a] presented the results of a temperature-dependent Mössbauer investigation of the $[Fe_4(S_2C_2(CF_3)_2)_4(\mu_3\text{-}S)_4]^n$ series ($n = 0, -1, -2$ as the $[AsPh_4]^+$ salts); this zero-(applied field) spectral study was shortly followed by magnetic-field Mössbauer measurements of these compounds by Reiff and co-workers.[5b] Room-temperature Mössbauer spectra performed by Künding on members of both series were reported earlier by Balch.[4] These Mössbauer data are of special importance with respect to the nature of bonding of these particular Fe_4S_4 clusters (vide infra).

(b) The Fe_4S_4 Fragment. This structural determination ascertained that the Fe_4S_4 core experimentally conforms to a tetragonal D_{2d}—$\bar{4}2m$ geometry. Table II shows that the six Fe–Fe distances in the iron tetrahedron separate under this symmetry into *four* shorter equivalent lengths of range 2.713 (7)–2.738 (7) Å and mean 2.730 Å and *two* longer equivalent lengths of range 3.222 (7)–3.225 (7) Å and mean 3.224 Å. Likewise, the six S···S distances in the nonbonding sulfur tetrahedron divide into *two* shorter equivalent lengths of range 2.844 (12)–2.866 (13) Å and mean 2.855 Å and *four* longer equivalent lengths of range 3.437 (13)–3.446 (13) Å and mean 3.442 Å. These variations correspond to the iron tetrahedron being uniformly compressed via Fe–Fe bonding (vide infra) along the S_4—$\bar{4}$ axis from a nonbonding cubic T_d geometry into a tetragonal D_{2d} geometry. This distortion concomitantly gives rise to an expansion of the four equivalent S···S edges (bisecting the Fe–Fe bonds) relative to the other two S···S edges perpendicular to the S_4 axis.

The *four* equivalent Fe–S bonds, which are approximately parallel to the S_4 axis, of range 2.150 (11)–2.155 (10) Å and mean 2.153 Å are markedly longer by 0.09 Å than the other *eight* equivalent Fe–S bonds of range 2.235 (10)–2.257 (10) Å and mean 2.247 Å. This bond-length difference may be ascribed to the particular electronic nature of the Fe_4S_4 core in the dianion (vide infra).

These observed bond-length variations expectedly produce correspondingly large separations of the 12 Fe–S–Fe and 12 S–Fe–S bond angles into two sets each. The *four* equivalent (Fe–Fe)-bonded Fe_2S_2 fragments possess *eight* acute Fe–S–Fe bond angles of 76.7° (average) and *eight* obtuse S–Fe–S bond angles of 102.9° (average), while the *two* equivalent (Fe–Fe)-nonbonded Fe_2S_2 fragments have *four* obtuse Fe–S–Fe bond angles of 91.7° (average) and *four* acute S–Fe–S bond angles of 78.9° (average). In contradistinction to each of the four (Fe–Fe)-bonded Fe_2S_2 fragments being essentially planar with a torsional angle θ of 171.4° (average) (i.e., the mean of 171.4, 171.4, 171.6, and 171.0°) along the Fe–Fe line between the two planes each formed by one bridging S atom and the two Fe atoms, the two (Fe–Fe)-nonbonded Fe_2S_2 fragments are each markedly nonplanar as indicated by corresponding torsional angles of θ = 131.3 and 131.8°.

This geometry of the Fe_4S_4 core in the $[Fe_4(S_2C_2(CF_3)_2)_4(\mu_3\text{-}S)_4]^{2-}$ dianion resembles that of the Fe_4S_4 core in the $[Fe_4(\eta^5\text{-}C_5H_5)_4(\mu_3\text{-}S)_4]^{2+}$ dication (vide infra) in sharp contrast to the different geometries of the Fe_4S_4 cores in other structurally known $[Fe_4L_4(\mu_3\text{-}S)_4]^n$ tetramers (viz., L = C_5H_5, $n = 0$,[1] 1[2]; L = SR, $n = -2, -3$;[6] L = Cl, $n = -2$;[7] L = NO, $n = 0, -1$;[8] L = $(CO)_3$, $n = 0$[9]).

(c) The Dithiolene Ligands and Their Arrangement about the Fe_4S_4 Core. Figures 1 and 2 show the disposition of the four $S_2C_2(CF_3)_2$ ligands about the central Fe_4S_4 framework. This particular ligand arrangement results in each of the four chemically equivalent iron atoms adopting a localized square-pyramidal sulfur coordination. Figure 3 depicts the localized environment about one of the iron atoms, while Table IV presents the appropriate bond angles and S···S contacts in its coordination sphere. These distances and bond angles are averaged under assumed S_4—$\bar{4}$ symmetry for the entire dianion. The fact that each iron atom is displaced by 0.60 Å (average) from its mean basal plane

---

[21] Schrauzer, G. N.; Mayweg, V. P.; Finck, H. W.; Henrich, W. *J. Am. Chem. Soc.* **1966**, *88*, 4604–4609.

Table II. Interatomic Distances (Å) and Bond Angles (Deg) for $[AsPh_4]_2^+[Fe_4(S_2C_2(CF_3)_2)_4(\mu_3\text{-}S)_4]^{2-}$

A. Intraanion Distances and Bond Angles within the $Fe_4(\mu_3\text{-}S)_4$ Core (Averaged under Assumed $D_{2d}-\bar{4}2m$ Symmetry)

Fe(1)–Fe(3)	2.731 (7)	Fe(1)–S(1)	2.246 (10)	S(1)···S(3)	3.444 (13)	Fe(1)–S(3)	2.153 (11)
Fe(1)–Fe(4)	2.713 (7)	Fe(1)–S(2)	2.257 (10)	S(1)···S(4)	3.437 (13)	Fe(2)–S(4)	2.155 (10)
Fe(2)–Fe(3)	2.738 (7)	Fe(2)–S(1)	2.249 (10)	S(2)···S(3)	3.446 (13)	Fe(3)–S(2)	2.153 (11)
Fe(2)–Fe(4)	2.737 (7)	Fe(2)–S(2)	2.251 (10)	S(2)···S(4)	3.439 (13)	Fe(4)–S(1)	2.150 (11)
average	2.730	Fe(3)–S(3)	2.245 (10)	average	3.442	average	2.153
Fe(1)···Fe(2)	3.225 (7)	Fe(3)–S(4)	2.246 (10)	S(1)···S(2)	2.866 (13)		
Fe(3)···Fe(4)	3.222 (7)	Fe(4)–S(3)	2.235 (10)	S(3)···S(4)	2.844 (12)		
average	3.224	Fe(4)–S(4)	2.246 (10)	average	2.855		
		average	2.247				
Fe(1)–S(2)–Fe(3)	76.5 (4)	Fe(1)–S(1)–Fe(2)	91.7 (4)	S(1)–Fe(1)–S(3)	103.0 (4)	S(1)–Fe(1)–S(2)	79.1 (4)
Fe(1)–S(3)–Fe(3)	76.7 (3)	Fe(1)–S(2)–Fe(2)	91.3 (4)	S(1)–Fe(4)–S(3)	103.5 (4)	S(1)–Fe(2)–S(2)	79.1 (4)
Fe(2)–S(2)–Fe(3)	76.8 (4)	Fe(3)–S(3)–Fe(4)	92.0 (3)	S(2)–Fe(1)–S(3)	102.8 (4)	S(3)–Fe(3)–S(4)	78.6 (4)
Fe(2)–S(4)–Fe(3)	76.9 (3)	Fe(3)–S(4)–Fe(4)	91.6 (4)	S(2)–Fe(3)–S(3)	103.2 (4)	S(3)–Fe(4)–S(4)	78.8 (4)
Fe(2)–S(1)–Fe(4)	76.9 (4)	average	91.7	S(2)–Fe(2)–S(4)	102.6 (4)	average	78.9
Fe(2)–S(4)–Fe(4)	76.9 (3)			S(2)–Fe(3)–S(4)	102.8 (4)		
Fe(1)–S(1)–Fe(4)	76.2 (4)			S(1)–Fe(2)–S(4)	102.6 (4)		
Fe(1)–S(3)–Fe(4)	76.4 (3)			S(1)–Fe(4)–S(4)	102.8 (4)		
average	76.7			average	102.9		

B. Intraanion Distances within Each $Fe(S_2C_2(CF_3)_2)$ Fragment

Fe(1)–S(11)	2.182 (10)	C(11)–C(13)	1.55 (6)	S(11)–C(11)	1.75 (4)	C(13)–F(1)	1.26 (6)
Fe(1)–S(12)	2.150 (10)	C(12)–C(14)	1.53 (6)	S(12)–C(12)	1.76 (3)	C(13)–F(2)	1.29 (6)
Fe(2)–S(21)	2.176 (11)	C(21)–C(23)	1.48 (5)	S(21)–C(21)	1.74 (3)	C(13)–F(3)	1.26 (6)
Fe(2)–S(22)	2.174 (10)	C(22)–C(24)	1.61 (4)	S(22)–C(22)	1.70 (3)	C(14)–F(4)	1.31 (5)
Fe(3)–S(31)	2.186 (10)	C(31)–C(33)	1.57 (6)	S(31)–C(31)	1.69 (3)	C(14)–F(5)	1.21 (5)
Fe(3)–S(32)	2.180 (10)	C(32)–C(34)	1.49 (5)	S(32)–C(32)	1.75 (3)	C(14)–F(6)	1.39 (5)
Fe(4)–S(41)	2.181 (11)	C(41)–C(43)	1.70 (7)	S(41)–C(41)	1.66 (3)	C(23)–F(7)	1.37 (4)
Fe(4)–S(42)	2.155 (10)	C(42)–C(44)	1.45 (6)	S(42)–C(42)	1.69 (3)	C(23)–F(8)	1.40 (4)
average	2.173	average	1.55	average	1.72	C(23)–F(9)	1.29 (4)
S(11)···S(12)	3.031 (14)			C(11)–C(12)	1.32 (4)	C(24)–F(10)	1.28 (4)
S(21)···S(22)	3.031 (13)			C(21)–C(22)	1.30 (4)	C(24)–F(11)	1.37 (4)
S(31)···S(32)	3.052 (13)			C(31)–C(32)	1.37 (4)	C(24)–F(12)	1.30 (4)
S(41)···S(42)	3.005 (14)			C(41)–C(42)	1.40 (4)	C(33)–F(13)	1.26 (6)
average	3.030			average	1.35	C(33)–F(14)	1.32 (6)
						C(33)–F(15)	1.27 (6)
						C(34)–F(16)	1.36 (5)
						C(34)–F(17)	1.35 (5)
						C(34)–F(18)	1.38 (5)
						C(43)–F(19)	1.03 (6)
						C(43)–F(20)	1.43 (6)
						C(43)–F(21)	1.23 (6)
						C(44)–F(22)	1.34 (5)
						C(44)–F(23)	1.25 (5)
						C(44)–F(24)	1.37 (5)

C. Intraanion Bond Angles within Each $Fe(S_2C_2(CF_3)_2)$ Fragment

S(11)–Fe(1)–S(12)	88.8 (4)	S(11)–C(11)–C(12)	117 (3)	C(11)–C(13)–F(1)	110 (5)	F(1)–C(13)–F(2)	111 (6)
S(21)–Fe(2)–S(22)	88.3 (4)	S(12)–C(12)–C(11)	121 (3)	C(11)–C(13)–F(2)	111 (5)	F(1)–C(13)–F(3)	108 (6)
S(31)–Fe(3)–S(32)	88.7 (4)	S(21)–C(21)–C(22)	119 (3)	C(11)–C(13)–F(3)	111 (5)	F(2)–C(13)–F(3)	106 (5)
S(41)–Fe(4)–S(42)	87.8 (4)	S(22)–C(22)–C(21)	122 (3)	C(12)–C(14)–F(4)	113 (4)	F(4)–C(14)–F(5)	111 (5)
average	88.4	S(31)–C(31)–C(32)	121 (3)	C(12)–C(15)–F(5)	119 (5)	F(4)–C(14)–F(6)	96 (4)
Fe(1)–S(11)–C(11)	106.9 (13)	S(32)–C(32)–C(31)	117 (3)	C(12)–C(16)–F(6)	110 (4)	F(5)–C(14)–F(6)	105 (5)
Fe(1)–S(12)–C(12)	105.6 (12)	S(41)–C(41)–C(42)	120 (4)	C(21)–C(23)–F(7)	114 (4)	F(7)–C(23)–F(8)	102 (3)
Fe(2)–S(21)–C(21)	105.5 (12)	S(42)–C(42)–C(41)	118 (3)	C(21)–C(23)–F(8)	112 (3)	F(7)–C(23)–F(9)	106 (4)
Fe(2)–S(22)–C(22)	105.3 (11)	average	119	C(21)–C(23)–F(9)	119 (4)	F(8)–C(23)–F(9)	102 (3)
Fe(3)–S(31)–C(31)	106.5 (13)	C(11)–C(12)–C(14)	121 (4)	C(22)–C(24)–F(10)	112 (3)	F(10)–C(24)–F(11)	107 (3)
Fe(3)–S(32)–C(32)	106.3 (12)	C(12)–C(11)–C(13)	127 (4)	C(22)–C(24)–F(11)	110 (3)	F(10)–C(24)–F(12)	113 (4)
Fe(4)–S(41)–C(41)	107.0 (11)	C(21)–C(22)–C(24)	123 (3)	C(22)–C(24)–F(12)	111 (3)	F(11)–C(24)–F(12)	104 (3)
Fe(4)–S(42)–C(42)	107.7 (13)	C(22)–C(21)–C(23)	130 (4)	C(31)–C(33)–F(13)	115 (5)	F(13)–C(33)–F(14)	104 (5)
average	106.4	C(31)–C(32)–C(34)	127 (4)	C(31)–C(33)–F(14)	108 (5)	F(13)–C(33)–F(15)	112 (6)
S(11)–C(11)–C(13)	116 (3)	C(32)–C(31)–C(33)	123 (4)	C(31)–C(33)–F(15)	110 (5)	F(14)–C(33)–F(15)	107 (6)
S(12)–C(12)–C(14)	117 (3)	C(41)–C(42)–C(44)	128 (4)	C(32)–C(34)–F(16)	114 (4)	F(16)–C(34)–F(17)	107 (4)
S(21)–C(21)–C(23)	112 (3)	C(42)–C(41)–C(43)	120 (2)	C(32)–C(34)–F(17)	114 (4)	F(16)–C(34)–F(18)	104 (4)
S(22)–C(22)–C(24)	115 (2)	average	125	C(32)–C(34)–F(18)	110 (5)	F(17)–C(34)–F(18)	108 (4)
S(31)–C(31)–C(33)	116 (3)			C(41)–C(43)–F(19)	119 (5)	F(19)–C(43)–F(20)	108 (4)
S(32)–C(32)–C(34)	115 (3)			C(41)–C(43)–F(20)	95 (5)	F(19)–C(43)–F(21)	135 (6)
S(41)–C(41)–C(43)	120 (3)			C(41)–C(43)–F(21)	99 (5)	F(20)–C(43)–F(21)	90 (6)
S(42)–C(42)–C(44)	114 (3)			C(42)–C(44)–F(22)	117 (5)	F(22)–C(44)–F(23)	102 (5)
average	116			C(42)–C(44)–F(23)	122 (5)	F(22)–C(44)–F(24)	99 (5)
				C(42)–C(44)–F(24)	114 (5)	F(23)–C(44)–F(24)	100 (5)
				average	112	average	106

D. Intraanion Distances and Bond Angles between the $Fe_4(\mu_3\text{-}S)_4$ Core and Four $Fe(S_2C_2(CF_3)_2)$ Fragments in the Resulting $Fe_4(S_2)_4(\mu_3\text{-}S)_4$ Moiety (Averaged under Assumed $S_4-\bar{4}$ Symmetry)

S(11)···S(1)	3.073 (13)	S(11)–Fe(1)–Fe(4)	94.2 (3)	S(12)···S(2)	3.064 (13)	S(12)–Fe(1)–Fe(3)	99.3 (3)
S(21)···S(2)	3.096 (13)	S(21)–Fe(2)–Fe(3)	94.4 (3)	S(22)···S(1)	3.073 (13)	S(22)–Fe(2)–Fe(4)	100.0 (3)
S(31)···S(3)	3.094 (14)	S(31)–Fe(3)–Fe(1)	96.0 (3)	S(32)···S(4)	3.026 (13)	S(32)–Fe(3)–Fe(2)	99.0 (3)
S(41)···S(4)	3.087 (14)	S(41)–Fe(4)–Fe(2)	96.5 (3)	S(42)···S(3)	3.005 (13)	S(42)–Fe(4)–Fe(1)	99.3 (3)
average	3.088	average	95.3	average	3.042	average	99.4

Table II (*Continued*)

S(11)· · ·S(3)	3.434 (13)	S(11)–Fe(1)–S(2)	151.5 (4)	S(12)· · ·S(3)	3.540 (14)	S(12)–Fe(1)–S(1)	145.8 (5)
S(21)· · ·S(4)	3.410 (13)	S(21)–Fe(2)–S(1)	152.7 (5)	S(22)· · ·S(4)	3.582 (14)	S(22)–Fe(2)–S(2)	145.3 (4)
S(31)· · ·S(2)	3.468 (14)	S(31)–Fe(3)–S(4)	150.4 (4)	S(32)· · ·S(2)	3.602 (14)	S(32)–Fe(3)–S(3)	143.6 (4)
S(41)· · ·S(1)	3.473 (14)	S(41)–Fe(4)–S(3)	149.2 (5)	S(42)· · ·S(1)	3.585 (14)	S(42)–Fe(4)–S(4)	143.7 (4)
average	3.446	average	151.0	average	3.577	average	144.6
S(11)–Fe(1)–S(1)	87.9 (4)	S(11)–Fe(1)–Fe(3)	157.9 (4)	S(12)–Fe(1)–S(2)	88.1 (4)	S(12)–Fe(1)–Fe(4)	163.9 (4)
S(21)–Fe(2)–S(2)	88.7 (4)	S(21)–Fe(2)–Fe(4)	156.9 (4)	S(22)–Fe(2)–S(1)	88.0 (4)	S(22)–Fe(2)–Fe(3)	164.7 (4)
S(31)–Fe(3)–S(3)	88.6 (4)	S(31)–Fe(3)–Fe(2)	159.3 (4)	S(32)–Fe(3)–S(4)	86.2 (4)	S(32)–Fe(3)–Fe(1)	165.9 (4)
S(41)–Fe(4)–S(4)	88.4 (4)	S(41)–Fe(4)–Fe(1)	160.1 (4)	S(42)–Fe(4)–S(3)	86.4 (4)	S(42)–Fe(4)–Fe(2)	166.0 (4)
average	88.4	average	158.6	average	87.3	average	165.1
S(11)–Fe(1)–S(3)	104.8 (4)			S(12)–Fe(1)–S(3)	110.7 (4)		
S(21)–Fe(2)–S(4)	103.9 (4)			S(22)–Fe(2)–S(4)	111.7 (4)		
S(31)–Fe(3)–S(2)	106.1 (4)			S(32)–Fe(3)–S(2)	112.5 (4)		
S(41)–Fe(4)–S(1)	106.6 (4)			S(42)–Fe(4)–S(1)	112.8 (4)		
average	105.4			average	111.9		
E. Interatomic Distances and Bond Angles within the Two Tetraphenylarsonium Cations							
As(1)–C(1-1)	1.906	C(1-1)–As(1)–C(2-1)	109.4	As(2)–C(5-1)	1.890	C(5-1)–As(2)–C(6-1)	106.4
As(1)–C(2-1)	1.853	C(1-1)–As(1)–C(3-1)	109.7	As(2)–C(6-1)	1.905	C(5-1)–As(2)–C(7-1)	112.6
As(1)–C(3-1)	1.913	C(1-1)–As(1)–C(4-1)	111.0	As(2)–C(7-1)	1.882	C(5-1)–As(2)–C(8-1)	107.0
As(1)–C(4-1)	1.883	C(2-1)–As(1)–C(3-1)	107.5	As(2)–C(8-1)	1.889	C(6-1)–As(2)–C(7-1)	109.5
average	1.889	C(2-1)–As(1)–C(4-1)	110.5	average	1.892	C(6-1)–As(2)–C(8-1)	113.4
		C(3-1)–As(1)–C(4-1)	108.6			C(7-1)–As(2)–C(8-1)	108.1
		average	109.5			average	109.5

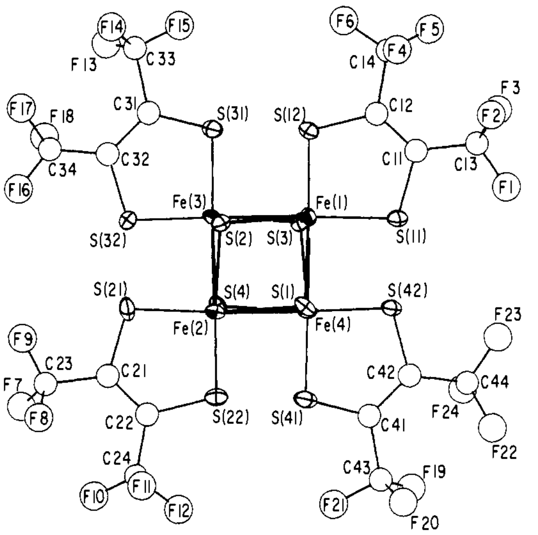

Figure 2. View down the pseudo-S_4—$\bar{4}$ axis of the $[Fe_4(S_2C_2(CF_3)_2)_4(\mu_3\text{-}S)_4]^{2-}$ dianion.

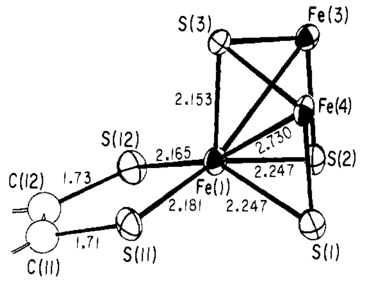

Figure 3. Observed square-pyramidal sulfur environment about one of the four chemically equivalent iron atoms in the $[Fe_4(S_2C_2(CF_3)_2)_4(\mu_3\text{-}S)_4]^{2-}$ dianion. S(3) is the axial ligand, while S(1), S(2), S(11), and S(12) are the basal ligands about Fe(1). Fe(1)–Fe(4) and Fe(1)–Fe(3) bonds effectively bisect the S(1)–Fe(1)–S(3) and S(2)–Fe(1)–S(3) bond angles, respectively. Bond lengths given here are averaged under assumed S_4—$\bar{4}$ symmetry. Each iron atom is located 0.60 Å (average) above the mean basal sulfur plane toward its axial ligand.

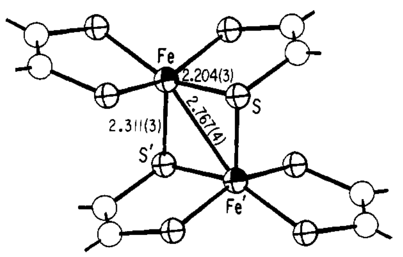

Figure 4. Configuration of the $Fe_2(S_2C_2)_4$ fragment of the $[Fe_2(S_2C_2(CF_3)_2)_4]^-$ monoanion[23] which possesses crystallographic C_i—$\bar{1}$ site symmetry. The basic architecture for this $[M_2(S_2X)_4]^n$ dimer (M = Fe, Co) may be considered as arising from a centrosymmetric dimerization of two identical $M(S_2X)_2$ units via the formation of two $M\text{–}S_A$ linkages to give a central planar M_2S_2 fragment. For the iron and cobalt dimers (Table V) possessing π-acidic dithiolene ligands,[23,24,29,30] each centrosymmetrically related metal atom possesses a localized square-pyramidal sulfur environment in contrast to an observed distorted trigonal-bipyramidal sulfur environment found when the chelating sulfur ligands are either ethane-1,2-dithiolate[25] or dithiocarbamate.[26] The similar Fe–Fe distances for the corresponding Fe_2S_2 fragments in the $[Fe_2(S_2C_2(CF_3)_2)_4]^-$ monoanion (2.767 (4) Å) and the $[Fe_4(S_2C_2(CF_3)_2)_4(\mu_3\text{-}S)_4]^{2-}$ dianion (2.730 Å (average) for the four equivalent Fe_2S_2 rings of the Fe_4S_4 core), which have the same geometrically disposed $S_2C_2(CF_3)_2{}^{2-}$ ligands and an identical average $d^{4.5}$ Fe(+3.5) valency for each iron atom, provide definite evidence for the existence of direct Fe–Fe interactions in both complexes.

of four S_B atoms toward its axial S_A atom results in four obtuse $S_A\text{–Fe–}S_B$ bond angles which vary from 105 to 112°. Three of the four $S_B\text{–Fe–}S_B$ bond angles are within 1° of 88°, with the fourth angle being 9° less due to the angular constraint imposed by one of the two (Fe–Fe)-nonbonded Fe_2S_2 fragments of the Fe_4S_4 core.[22]

This close conformity of the five sulfur atoms about each iron atom to a square-pyramidal configuration necessitates that all of the sulfur atoms lie essentially in two planar layers (Figure 2) which are separated from each other by ca. 3.1 Å. Each layer consists of six sulfur atoms whose arrangement may be envisioned as two fused sulfur squares with their common edge being the two triply bridging sulfur atoms from an (Fe–Fe)-nonbonded Fe_2S_2 fragment of the Fe_4S_4 core. These two parallel layers are perpendicularly oriented and symmetry related to each other by the pseudo S_4—$\bar{4}$ axis of the dianion. The four central sulfur atoms in these two layers form an elongated tetrahedron along the S_4 axis. The interpenetrating iron tetrahedron, which is compressed along the S_4 axis, arises from the iron atoms occupying all four

---

[22] The other two relatively short $S_B \cdots S_B$ contacts of 2.855 Å (average) and 3.030 Å (average) are mainly dictated by the "bite" within an (Fe–Fe)-nonbonded Fe_2S_2 fragment and within each bidentate $S_2C_2(CF_3)_2$ ligand, respectively.

Table III. Least-Squares Planes for the $[Fe_4(S_2C_2(CF_3)_2)_4(\mu_3\text{-}S)_4]^{2-}$ Dianion

A. Equations Defining Least-Squares Planes[a]

1. Plane through Fe(1), Fe(2), S(1)

$0.1036X + 0.8625Y - 0.4954Z - 8.9049 = 0$

2. Plane through Fe(1), Fe(2), S(2)

$-0.6018X + 0.7938Y - 0.0881Z - 7.2879 = 0$

3. Plane through Fe(3), Fe(4), S(3)

$0.0716X - 0.966Y - 0.0412Z + 13.3918 = 0$

4. Plane through Fe(3), Fe(4), S(4)

$-0.4253X + 0.6577Y - 0.6217Z - 0.0694 = 0$

5. Plane through Fe(1), Fe(3), S(2)

$-0.9025X - 0.3999Y - 0.1602Z + 14.0644 = 0$

6. Plane through Fe(1), Fe(3), S(3)

$-0.9113X - 0.3053Y - 0.2764Z + 13.8754 = 0$

7. Plane through Fe(2), Fe(3), S(2)

$0.3276X - 0.1645Y - 0.9304Z + 7.8890 = 0$

8. Plane through Fe(2), Fe(3), S(4)

$0.2865X - 0.3076Y - 0.9074Z + 9.9653 = 0$

9. Plane through Fe(2), Fe(4), S(1)

$-0.9373X - 0.2903Y - 0.1931Z + 10.7736 = 0$

10. Plane through Fe(2), Fe(4), S(4)

$-0.8785X - 0.4199Y - 0.2280Z + 12.5677 = 0$

11. Plane through Fe(1), Fe(4), S(1)

$0.3630X - 0.2762Y - 0.8899Z + 11.1446 = 0$

12. Plane through Fe(1), Fe(4), S(3)

$0.2484X - 0.1883Y - 0.9502Z + 11.1954 = 0$

13. Plane through S(1), S(2), S(11), S(12)

$-0.2916X + 0.9166Y - 0.2736Z - 9.9574 = 0$

S(1)	0.053	S(11)	−0.050	Fe(1)	−0.59
S(2)	−0.053	S(12)	0.050		

14. Plane through S(1), S(2), S(21), S(22)

$-0.2464X + 0.8949Y - 0.3720Z - 9.010 = 0$

S(1)	−0.071	S(21)	−0.067	Fe(2)	−0.58
S(2)	0.071	S(22)	0.067		

15. Plane through S(3), S(4), S(31), S(32)

$-0.3036X + 0.8873Y - 0.3472Z - 5.9864 = 0$

S(3)	−0.061	S(31)	0.057	Fe(3)	0.62
S(4)	0.062	S(32)	−0.058		

16. Plane through S(3), S(4), S(41), S(42)

$-0.2505X + 0.9215Y - 0.2968Z - 7.2844 = 0$

S(3)	0.049	S(41)	0.045	Fe(4)	0.63
S(4)	−0.048	S(42)	−0.046		

17. Plane through Fe(1), Fe(2), S(3), S(4)

$0.8619X + 0.0858Y - 0.4997Z - 1.987 = 0$

Fe(1)	−0.001	Fe(3)	1.62	S(11)	−1.57
Fe(2)	0.001	Fe(4)	1.61	S(12)	1.45
S(3)	0.001	S(1)	−1.43	S(21)	1.55
S(4)	−0.001	S(2)	1.44	S(22)	−1.46

18. Plane through Fe(3), Fe(4), S(1), S(2)

$-0.4262X - 0.4181Y - 0.8022Z + 16.2178 = 0$

Fe(3)	0.002	Fe(1)	−1.61	S(31)	−1.54
Fe(4)	−0.002	Fe(2)	1.62	S(32)	1.50
S(1)	0.002	S(3)	−1.41	S(41)	1.52
S(2)	−0.002	S(4)	1.43	S(42)	−1.47

B. Angles (Deg) between Normals to Planes

plane	angle	plane	angle	plane	angle
1,2	48.2	7,8	8.6	13,14	6.3
3,4	131.3	9,10	8.4	15,16	4.6
5,6	8.6	11,12	9.0	17,18	90.1

[a] The equations of the planes are given in an angstrom orthogonal coordinate system (X, Y, Z), which is related to the monoclinic crystallographic fractional coordinates (x, y, z) by the transformations: $X = ax + (c \cos\beta)z$, $Y = by$, $Z = (c \sin\beta)z$. Unit weights were used in the calculations of the planes.

Table IV. Observed Coordination Angles and Sulfur···Sulfur Separations about a Chemically Equivalent Iron Atom (Fe(1)), for Which Its Five Sulfur Ligands Approximately Conform to a Square-Pyramidal Configuration[a]

A. Bond Angles (Deg)

S_B–Fe–S_B	value[b]	S_A–Fe–S_B	value[b]
S(1)–Fe(1)–S(2)	78.9	S(3)–Fe(1)–S(1)	102.9
S(11)–Fe(1)–S(12)	88.4	S(3)–Fe(1)–S(2)	102.9
S(1)–Fe(1)–S(11)	88.4	S(3)–Fe(1)–S(11)	105.4
S(2)–Fe(1)–S(12)	87.3	S(3)–Fe(1)–S(12)	111.9

B. Distances (Å)

S_B···S_B	value[b]	S_A···S_B	value[b]
S(1)···S(2)	2.855	S(3)···S(1)	3.442
S(11)···S(12)	3.030	S(3)···S(2)	3.442
S(1)···S(11)	3.088	S(3)···S(11)	3.446
S(2)···S(12)	3.042	S(3)···S(12)	3.577

[a] The one axial sulfur atom (S(3)) and four basal sulfur atoms (S(1), S(2), S(11), S(12)) are designated by A and B, respectively. [b] Each of the given values has been averaged under assumed S_4–$\bar{4}$ symmetry for the entire dianion.

square-pyramidal holes between the two sulfur layers.

Other crystallographically determined complexes with a localized square-pyramidal sulfur environment about an iron atom include two structurally related iron dithiolene dimers, viz., the $[Fe_2(S_2C_2(CF_3)_2)_4]^-$ monoanion[23] and the $[Fe_2(S_2C_2(CN)_2)_4]^{2-}$ dianion.[24] The basic configuration of these iron dithiolene dimers is described in Figure 4. Two other analogously formed iron bis(sulfur chelate) dimers, the $[Fe_2(S_2C_2H_4)_4]^{2-}$ dianion[25] and $Fe_2(S_2CNEt_2)_4$,[26] containing non(π acidic) ethane-1,2-dithiolate and dithiocarbamate ligands, respectively, each possess a distorted trigonal-bipyramidal sulfur arrangement about each iron atom.

An examination of appropriate distances and bond angles as well as selected least-squares planes (Table III) reveals a breakdown of the dianion's symmetry from the experimentally found D_{2d} geometry for the Fe_4S_4 core to an approximate S_4 geometry. This is a consequence of a small but significant angular distortion of the two basal dithiolene sulfur atoms about a given iron atom from planarity with the other two basal sulfur atoms of the Fe_4S_4 core. This sterically induced deformation primarily involves a 3–4° twisting of the two basal dithiolene sulfur atoms about an axis bisecting both these two atoms and the other two basal sulfur atoms in order to increase the close S_B···S_B distances between each dithiolene ligand and the Fe_4S_4 core.[22] The extent of this angular deformation which relieves intraanionic overcrowding of the sulfur atoms is indicated by a mean difference

---

(23) Schultz, A. J.; Eisenberg, R. *Inorg. Chem.* **1973**, *12*, 518–525.
(24) Hamilton, W. C.; Bernal, I. *Inorg. Chem.* **1967**, *6*, 2003–2008.

Table V. Comparison of Selected Mean Geometrical Parameters for the Four (Fe–Fe)-Bonded Fe_2S_2 Rings of the Dianion with Those for Several $[M_2(S_2X)_4]^n$ Dimers (M = Fe, Co) Containing Planar M_2S_2 Rings

A. Bis(1,2-dithiolene) Complexes of Iron and Cobalt Containing a Square-Pyramidal Sulfur Coordination about Each Metal Atom

		ring dist, Å				ring angles, deg		
	av metal Ox state	M-(B.P.)[c]	M–M	M–S_A	M–S_B	S–M–S	M–S–M	ref
$[Fe_4(S_2C_2(CF_3)_2)_4(\mu_3\text{-}S)_4]^{2-}$	$d^{4.5}$ Fe(+3.5)[a,b]	0.60	2.730	2.153	2.247	102.9	78.9	this work
$[Fe_2(S_2C_2(CF_3)_2)_4]^-$	$d^{4.5}$ Fe(+3.5)[a,b]	0.43	2.767	2.311	2.204	104.5	75.6	23
$[Fe_2(S_2C_2(CN)_2)_4]^{2-}$	d^5 Fe(+3)[b]	0.36	3.07	2.46	2.28	99	81	24
$[Co_2(S_2C_2(CF_3)_2)_4$	d^5 Co(+4)[b]	0.37	2.781	2.382	2.156	99.7	80.3	29
$[Co_2(S_2C_6Cl_4)_4]^{2-}$	d^6 Co(+3)[b]	0.26	3.099	2.404	2.184	95.2	84.8	30

B. Complexes Containing a Distorted Trigonal-Bipyramidal Sulfur Coordination about Each Iron Atom

	av iron Ox state	Fe···Fe	Fe–S_A[d]	Fe–S_B[d]	S–Fe–S	Fe–S–Fe	ref
$[Fe_2(S_2C_2H_4)_4]^{2-}$	d^5 Fe(+3)	3.410	2.503	2.265	88.8	91.2	25
$Fe_2(S_2(NEt_2)_4$	d^6 Fe(+2)	3.350	2.437	2.613	97.2	82.8	26

[a] Equivalent metal atoms with average nonintegral oxidation states are based upon Mössbauer data showing no evidence for mixed-iron valency. [b] Predicated on the basis of each dithiolene ligand being regarded as a dianion. [c] Perpendicular displacement of the metal atom above the mean square-pyramidal plane of four basal S_B atoms toward the axial S_A atom. [d] Here, S_B denotes the basal Fe_2S_2-ring sulfur atom of the dithioline ligand chelating an iron atom, while S_A denotes the axial Fe_2S_2-ring sulfur atom of a different dithiolene ligand.

of 0.13 Å between the two $S_A \cdots S_B$(dithiolene) distances (which would be equivalent under assumed D_{2d} symmetry) as well as by the resulting nonequivalence of the two S_A–Fe–S(dithiolene) bond angles of 105.4° (average) and 111.9° (average). Table III also shows a small but definite bending of the essentially planar $S_2C_2C_2$ part of each dithiolene ring out of the FeS_2(dithiolene) plane. This latter kind of deformation was also observed[24] for each dithiolene ring in the $[Fe_2(S_2C_2(CN)_2)_4]^{2-}$ dimer. Interactions among the four dithiolene ligands within the $[Fe_4(S_2C_2(CF_3)_2)_4(\mu_3\text{-}S)_4]^{2-}$ dianion appear not to be an important steric factor in that the four nearest-neighbor S···S separations, which range from 3.39 (1) to 3.51 (1) Å, are relatively long.

The two slightly different mean values (under S_4 symmetry) of 2.165 and 2.181 Å for the Fe–S(dithiolene) bond lengths are expectedly analogous to the corresponding ones found for the $S_2C_2(CF_3)_2$ ligands in the $[Fe_2(S_2C_2(CF_3)_2)_4]^-$ monoanion (2.175 Å (average))[23] and in $Fe(S_2C_2(CF_3)_2)(S_2CNEt_2)_2$ (2.195 Å (average)).[27] The relative shortness of these values may be readily attributed to an extensive π-electron delocalization between the Fe atom and $S_2C_2(CF_3)_2$ ligand system. Other bond parameters within each $S_2C_2(CF_3)_2$ ligand also agree within experimental error with those found[23,27,28] in previous structural determinations.

(d) Structural Relationship with the $[Fe_2(S_2C_2(CF_3)_2)_4]^-$ Monoanion and Other $[M_2(S_2X)_4]^n$ Dimers (M = Fe, Co) Containing Planar Fe_2S_2 Rings. A geometrical comparison (Table V) of the relevant fragments of the Fe_4S_4 core in the $[Fe_4(S_2C_2(CF_3)_2)_4(\mu_3\text{-}S)_4]^{2-}$ dianion with the Fe_2S_2 fragment possessed by four structurally determined $[Fe_2(S_2X)_4]^n$ dimers (where X denotes $C_2(CF_3)_2$, $n = -1$;[23] $C_2(CN)_2$, $n = -2$;[24] C_2H_4, $n = -2$;[25] $CNEt_2$, $n = 0$[26]) and two corresponding $[Co_2(S_2X)_4]^n$ dimers (where X designates $C_2(CF_3)_2$, $n = 0$;[29] and C_6Cl_4, $n = -2$[30]) is informative from a bonding viewpoint. Although each of the above six dimers, of which the $[Fe_2(S_2C_2(CF_3)_2)_4]^-$ monoanion is shown in Figure 4, is crystallographically constrained in the solid state on a center of symmetry to have a rigorously planar M_2S_2 ring, the localized coordination of the five sulfur atoms about each metal atom is a square pyramid for the two iron and two cobalt dithiolene complexes vs. a distorted trigonal bipyramid for the iron ethane-1,2-dithiolate and dithiocarbamate complexes. A salient structural feature is that the central M_2S_2 ring in each of the two iron and two cobalt dithiolene complexes may be considered as geometrically corresponding (relative to the terminal dithiolene ligands) to one of the four equivalent (Fe–Fe)-bonded Fe_2S_2 rings of the Fe_4S_4 core in the $[Fe_4(S_2C_2(CF_3)_2)_4(\mu_3\text{-}S)_4]^{2-}$ dianion. (Compare the orientation in Figure 4 of the Fe_2S_2 ring of the $[Fe_2(S_2C_2(CF_3)_2)_4]^-$ monoanion with that in Figure 1 of the Fe_2S_2 ring formed by the Fe(2), Fe(4), S(1), and S(4) atoms in the Fe_4S_4 core of the dianion.) Since the $[Fe_2(S_2C_2(CF_3)_2)_4]^-$ and $[Fe_4(S_2C_2(CF_3)_4(\mu_3\text{-}S)_4]^{2-}$ anions possess the same π-acidic $S_2C_2(CF_3)_2{}^{2-}$ ligands, the fact that the Fe–Fe bond length of 2.767 (6) Å in the Fe_2S_2 ring of the monoanion is analogous to that of 2.730 Å (average) in each of the four equivalent Fe_2S_2 rings of the Fe_4S_4 core of the dianion provides a definite indication for the existence of direct Fe–Fe interactions in both of these two complexes.

Unfortunately, an inspection of the distances and bond angles given (Table V) for the M_2S_2 ring of the structurally characterized iron and cobalt dithiolene dimers does not provide a clear-cut bonding interpretation of the observed changes in geometry upon variation of the number of metal valence electrons. One major problem is the lack of crystallographic data for all members of a given metal dithiolene series containing the same dithiolene ligands (e.g., $[Fe_2(S_2C_2(CF_3)_2)_4]^n$ with $n = 0, -1, -2$[30,31]); such information is needed in order to appraise in a systematic fashion the geometrical influence of oxidation and/or reduction. Nevertheless, the crystallographic data presented in Table V appear to be consistent with respect to the following stereochemical and bonding assessment which is based upon the premise that the particular size and shape adopted by a planar M_2S_2 ring in a given metal dithiolene dimer is dictated primarily by electronic effects. However, the existence of considerable nonbonding repulsion forces between adjacent dithiolene ligands in these dimers is indicated by the considerable directional displacements of the outer atoms in each dithiolene ligand from planarity.

The paramagnetic $[Fe_2(S_2C_2(CF_3)_2)_4]^-$ monoanion (a d^9 electron system with two $d^{4.5}$ Fe(+3.5)) and diamagnetic $Co_2(S_2C_2(CF_3)_2)_4$ molecule (a d^{10} electron system with two d^5 Co(+4)) possess metal–metal distances of 2.767 (4) and 2.781 (6) Å indicative of discrete metal–metal bonds. On the other hand, the $[Fe_2(S_2C_2(CN)_2)_4]^{2-}$ dianion (a d^{10} electron system with two d^5 Fe(+3)), which is antiferromagnetic with two spin components of $^1/_2$, has a longer metal–metal distance of 3.07 Å, thereby signifying a greatly reduced metal–metal interaction. The dia-

---

(25) Snow, M. R.; Ibers, J. A. *Inorg. Chem.* **1973**, *12*, 249–254.

(26) Ileperuma, O. A.; Feltham, R. D. *Inorg. Chem.* **1975**, *14*, 3042–3045.

(27) Johnston, D. L.; Rohrbaugh, W. L.; Horrocks, DeW., Jr. *Inorg. Chem.* **1971**, *10*, 1474–1479.

(28) Enemark, J. H.; Lipscomb, W. N. *Inorg. Chem.* **1965**, *4*, 1729–1734.

(29) Baker-Hawkes, M. J.; Dori, Z.; Eisenberg, R.; Gray, H. B. *J. Am. Chem. Soc.* **1968**, *90*, 4253–4259.

(30) The crystallographically determined monoanion is the first reduced member of an electron-transfer $[Fe_2(S_2C_2(CF_3)_2)_4]^n$ series (n = 0, −1, −2) whose spectral, magnetic, and electrochemical properties were reported by Balch, Dance, and Holm.[31] Magnetic moments of crystalline solids of the three members of this series were found to decrease with decreasing temperature, thereby reflecting antiferromagnetic coupling of spins between the two halves of each dimer. The detailed susceptibility data were interpreted[31] on the basis of a ground-state spin of $^1/_2$ for the monoanion and 0 for the neutral parent and dianion, with excited electronic states of spin degeneracy greater than that of the ground state being thermally populated in the 80–300 K range.

(31) Balch, A. L.; Dance, I. G.; Holm, R. H. *J. Am. Chem. Soc.* **1968**, *90*, 1139–1145.

Table VI. Selected Mean Distances (Å) and Bond Angles (Deg) for the Fe_4S_4 Cores in the $[Fe_4(S_2C_2(CF_3)_2)_4(\mu_3\text{-}S)_4]^{2-}$ Dianion and the $[Fe_4(\eta^5\text{-}C_5H_5)_4(\mu_3\text{-}S)_4]^{2+}$ Dication

tetramer	$[Fe_4\text{-}(S_2C_2(CF_3)_2)_4\text{-}(\mu_3\text{-}S)_4]^{2-}$	$[Fe_4\text{-}(\eta^5\text{-}C_5H_5)_4\text{-}(\mu_3\text{-}S)_4]^{2+}$
cryst site symmetry	$C_1-\bar{1}$	$S_4-\bar{4}$
idealized geometry of Fe_4S_4 core	$D_{2d}-\bar{4}2m$	$D_{2d}-\bar{4}2m$
Fe–Fe	[4][a] 2.730	[4] 2.834
	[2] 3.224	[2] 3.254
S···S	[2] 2.855	[2] 2.820
	[4] 3.442	[4] 3.304
Fe–S	[4] 2.153	[4] 2.156
	[8] 2.247	[8] 2.208
Fe–S–Fe	[8] 76.7	[8] 81.0
	[4] 91.7	[4] 94.9
S–Fe–S	[4] 78.9	[4] 79.3
	[8] 102.9	[8] 98.4

[a] Square brackets denote the number of distances or bond angles under assumed tetragonal D_{2d} symmetry having the values listed in the right column.

magnetic $[Co_2(S_2C_6Cl_4)_4]^{2-}$ dianion (a d^{12} electron system with two d^6 Co(+3)) expectedly has a nonbonding metal–metal distance of 3.099 (4) Å. These results indicate that the geometries of the M_2S_2 rings in these dimers are strongly influenced by the nature of the terminal and bridging dithiolene ligands and that metal–metal bonding is a contributory but not dominant effect. It is apparent that the π-acidic nature of the particular dithiolene ligand appears to govern the extent of dimerization which occurs via formation of the two equivalent $M\text{–}S_A$ bonds (i.e., those from a metal atom in one square-planar monomer to the sulfur atom of a dithiolene ring in the other monomer). Hence, the composite effects of a larger formal metal oxidation state (e.g., a d^9 vs. a d^{10} dimetal system) and stronger π-acidic ligands (e.g., $S_2C_2(CF_3)_2$ vs. $S_2C_2(CN)_2$) result in a decrease of charge density near the metal atoms and thereby favor dimerization through increased $S_A \rightarrow M$ and M–M interactions. Table V also reveals that the $M\text{–}S_A$ and M–M distances in the M_2S_2 rings depend upon the degree of displacement of each metal atom from its four basal sulfur atoms. These observed differences in geometry of the iron and cobalt dithiolene dimers may be rationalized on the basis of qualitative MO considerations which are deferred until additional crystallographic data on other dimers are available.

The different sulfur arrangement about each iron atom in the $[Fe_2(S_2C_2H_4)_4]^{2-}$ dianion[25] (a d^{10} electron system with two d^5 Fe(+3)) along with the nonbonding Fe···Fe separation of 3.410 (4) Å has been ascribed[23,25] to the non(π-acidic) character of the ethanedithiolate ligands. Likewise, the observed trigonal-bipyramidal distortion of the sulfur atoms about the iron atoms together with the abnormally long $Fe\text{–}S_B$ bond of 2.61 Å in the neutral $Fe_2(S_2CNEt_2)_4$ dimer,[26] which exhibits antiferromagnetic coupling of the two high-spin d^6 Fe(II), were attributed[26] in this case to the small "bite" angle of the dithiocarbamate ligands.

(e) Structural Relationship with the $[Fe_4(\eta^5\text{-}C_5H_5)_4(\mu_3\text{-}S)_4]^{2+}$ Dication and Resulting Electronic Implications. The prime incentive for this study was to obtain a precise configuration of the $[Fe_4(S_2C_2(CF_3)_2)_4(\mu_3\text{-}S)_4]^{2-}$ dianion in order to assess the mode of the Fe–Fe interactions in the Fe_4S_4 core. Table VI compares its mean parameters with those for the Fe_4S_4 core of the $[Fe_4(\eta^5\text{-}C_5H_5)_4(\mu_3\text{-}S)_4]^{2+}$ dication. The experimental conformity of the Fe_4S_4 core of the Balch dianion to a tetragonal D_{2d} geometry with both Fe–Fe and Fe–S distances paralleling those in the Fe_4S_4 core of the dication provides convincing evidence (in our minds) for analogous Fe–Fe interactions in these two clusters. These results are in complete harmony with the previously proposed qualitative metal cluster model[3] which assumes an 18-electron system for both the dication and dianion in order to achieve an iron tetrahedron with four short and two long Fe–Fe distances. The availability of an 18-electron tetrairon system, which for each complex formally corresponds to four $d^{4.5}$ Fe(+3.5), is based upon each cyclopentadienyl ligand being regarded as a monoanion and each sulfide and dithiolene ligand being regarded as a dianion.

Table VI also reveals that an analogous direct correlation exists in both the $[Fe_4(S_2C_2(CF_3)_2)_4(\mu_3\text{-}S)_4]^{2-}$ dianion and $[Fe_4(\eta^5\text{-}C_5H_5)_4(\mu_3\text{-}S)_4]^{2+}$ dication between the Fe–Fe and Fe–S distances for the six fused Fe_2S_2 fragments which make up the faces of the cubanelike Fe_4S_4 core. Each of the four vertical Fe–S bonds (approximately parallel to the S_4—$\bar{4}$ axis) along a common fused edge of two (Fe–Fe)-bonded Fe_2S_2 fragments is 0.09 Å (average) shorter than each of the other eight Fe–S bonds along a common fused edge of an (Fe–Fe)-bonded and an (Fe–Fe)-nonbonded Fe_2S_2 fragment. An analogous trend between Fe–S and Fe–Fe distances is also observed in the Fe_4S_4 cores of the other two structurally analyzed members (n = 0, 1) of the $[Fe_4(\eta^5\text{-}C_5H_5)_4(\mu_3\text{-}S)_4]^n$ series. This correlation provides definite evidence that Fe–Fe and Fe–S interactions in these Fe_4S_4 tetramers are not orthogonal to each other; the concomitant shortening of the relatively rigid Fe–S bonds in a given Fe_2S_2 fragment resulting from formation of Fe–Fe bonding within that fragment by a formal two-electron oxidation of an (Fe–Fe)-nonbonding fragment implies that the frontier MO from which the electrons are removed possesses both Fe–Fe and Fe–S antibonding orbital character.

Of particular interest is that zero-field Mössbauer spectra[5a] of the three members of the $[Fe_4(S_2C_2(CF_3)_2)_4(\mu_3\text{-}S)_4]^n$ series (n = 0, −1, −2) exhibit essentially identical temperature-independent quadrupole doublets with similar isomer shifts (ca. +0.1 mm/s relative to iron metal) and analogous quadrupole splittings (ca. 1.64 mm/s).[32,33] It was pointed out[5a] that the observed small increase of 0.03–0.04 mm/s in the isomer shift upon successive one-electron reductions is in accordance with a slightly lower s-electron density about the iron centers due presumably to increased d-electron shielding. These Mössbauer data were interpreted[5a] as evidence "that all iron sites in a given cluster are equivalent (or nearly so) with respect to their electronic environment" and that extensive delocalization occurs over the entire cluster. Subsequent Mössbauer spectra[5b] of the paramagnetic monoanion and of the diamagnetic neutral parent and dianion were obtained at 4.2 K in external magnetic fields (H_0) which varied from 40 to 65 kOe. From the observations that these spectra are all essentially identical with the effective field (H_n) at the iron nuclei being equal to H_0 for all values of H_0, it was concluded[5b] that the magnetic hyperfine field is ~0 and that the unpaired electron in the monoanion is completely delocalized on the ligands. The similarity of the Mössbauer spectra was then interpreted[5b] on the basis that reduction of the neutral parent "involves the additional electron(s) entering a MO composed equally and primarily of the dithiolene sulfur ligands".

Zero-field and high-field Mössbauer spectra reported by Reiff and co-workers[34] for the $[Fe_4(\eta^5\text{-}C_5H_5)_4(\mu_3\text{-}S)_4]^n$ series (n = 0, 1, 2) exhibit analogous single quadrupole doublets with virtually unchanged isomer shifts. Although Mössbauer spectroscopy is thereby not able to distinguish among the appreciably different Fe_4S_4 geometries of the three structurally analyzed members[1-3] of the above series, it can, however, readily discriminate[34] (via significant differences in isomer shifts and quadrupole splittings) between the $[Fe_4(\eta^5\text{-}C_5H_5)_4(\mu_3\text{-}S)_4]^{2+}$ dication and the $[Fe_4(C_2S_2(CF_3)_2)_4(\mu_3\text{-}S)_4]^{2-}$ dianion; nevertheless, their geometrically resembling Fe_4S_4 cores (ascertained herein) indicate closely related Fe–Fe interactions, even though there is a marked dissimilarity between these ions (because of their greatly different terminal

---

(32) The much greater quadrupole splittings observed in the Mössbauer spectra[33] for the square-pyramidal iron atoms of the $[Fe_2(S_2C_2(CN)_2)_4]^{2-}$ dimer (2.76 mm/s) and for the presumed square-pyramidal iron atoms of the $[Fe_2(S_2C_2(CF_3)_2)_4]^n$ dimers (2.4 mm/s for $n = 0$ and 2.4–2.5 mm/s for $n = -2$) may be largely a consequence of the considerable variation in the $Fe\text{–}S_A$ bond length (Table V) which is directly related to the extent of displacement of the iron atom above the mean plane of the four basal S_B atoms toward the axial S_A atom. A smaller $Fe\text{–}S_A$ bond length (corresponding to a larger displacement of the iron atom out of the mean S_B plane) is found in Table V to correlate directly with a smaller quadrupole splitting in accordance with the expectation that such a geometrical change should lead to a smaller electric field gradient at the iron nucleus.

(33) Birchall, T.; Greenwood, N. N. *J. Chem. Soc. A* **1969**, 286–291.

(34) Wong, H.; Sedney, D.; Reiff, W. M.; Frankel, R. B.; Meyer, T. J.; Salmon, D. *Inorg. Chem.* **1978**, *17*, 194–197.

ligands) in both the isomer shift, which measures the total s electron density at the iron nucleus, and the nuclear quadrupole splitting, which is a measure of the deviation from spherical symmetry of the electron density surrounding the iron nucleus.

Both the crystallographic analyses[1-3] and the resulting qualitative MO bonding model[3,8,35] for the $[Fe_4(\eta^5\text{-}C_5H_5)_4(\mu_3\text{-}S)_4]^n$ series support our premise that successive oxidations of the neutral $Fe_4(\eta^5\text{-}C_5H_5)_4(\mu_3\text{-}S)_4$ molecule ($n = 0$) to the monocation ($n = 1$) and dication ($n = 2$) involve the removal of the electron(s) from mainly a metal-based MO which has highly antibonding tetrairon orbital character rather than from ligand-based orbitals.[36-39] Furthermore, the observed invariance[34] of the Mössbauer isomer shift for the three isolated members ($n = 0, 1, 2$) of this series is a natural consequence of only a small "net" alteration in the d orbital electron population of the iron atoms upon oxidation due to the concomitantly greater localization of the other valence electrons from the ligands onto the iron atoms.

An analogous situation was previously shown to exist within the $[Fe_2(CO)_6(\mu_2\text{-}PR_2)_2]^n$ series ($n = 0, -1, -2$ for R = CH_3;[40] $n = 0, -2$ for R = Ph[41]), for which zero-field Mössbauer spectra[40] of the three dimethylphosphido-bridged dimers exhibited only small negative isomer shifts of 0.06–0.09 mm/s upon successive one-electron reductions. This small variation in Mössbauer isomer shifts was interpreted from our nonparameterized MO calculations[42] via the Fenske–Hall model[38] to reflect little alteration in the charge distribution of the iron atoms. Hence, although the additional electron(s) in the anions occupy a frontier molecular orbital that possesses large antibonding diiron orbital character, the iron atoms also act as charge transmitters which (in accordance with the electroneutrality principle) effectively dissipate the increased total charge density in the anions over the entire molecular system.[42] Direct experimental evidence that electron occupation of the lowest unoccupied molecular orbital (LUMO) of a neutral parent would completely rupture the Fe–Fe bond was subsequently furnished by a structural comparison[41] of the two-electron reduced diphenylphosphido-bridged dimer ($n = -2$) with that of the corresponding neutral dimer ($n = 0$). A dramatic geometrical change in the Fe_2P_2 core from a highly bent to a completely flattened configuration was observed on account of a resulting 1.0 Å increase in the Fe–Fe distance from a bonding value of 2.623 (2) Å in the parent ($n = 0$) to a nonbonding value of 3.630 (3) Å in the dianion ($n = -2$).[41]

The qualitative metal cluster bonding model previously invoked[3] for the $[Fe_4(\eta^5\text{-}C_5H_5)_4(\mu_3\text{-}S)_4]^{2+}$ dication assumes that the 18 d electrons available for direct Fe–Fe interactions occupy six bonding and three antibonding tetrametal symmetry orbitals. This gives rise to a total limiting valence bond order of 3.0 in the iron tetrahedron which has two long and four short Fe–Fe distances of 3.25 and 2.83 Å, respectively. The assumption that the two long Fe–Fe distances correspond to completely nonbonding interactions necessitates that each of the four shorter Fe–Fe distances corresponds to an Fe–Fe bond order of $^3/_4$, which is not inconsistent with these distances being ca. 0.2 Å longer than the two electron-pair Fe–Fe distances found in the neutral parent molecule.

Our structural evidence (Table VI) that the Fe_4S_4 core of the dianion may likewise be considered under this cluster model as an analogous 18-electron system allows one to predict probable geometrical changes expected for the other two isolated members ($n = 0, -1$) of the $[Fe_4(S_2C_2(CF_3)_2)_4(\mu_3\text{-}S)_4]^n$ series as well as for the corresponding members ($n = 0, -1, -2$) of the $[Fe_4(S_2C_2(CN)_2)_4(\mu_3\text{-}S)_4]^n$ series. The magnitudes of the proposed kinds of alterations obviously cannot be forecast, especially since the dithiolene ligands play an important role (as indicated from the electrochemical behavior[4] of the above two iron dithiolene series) in minimizing by appropriate charge flow marked changes in electron-charge distribution due to oxidation and/or reduction. The proposed differences in geometry for the Fe_4S_4 cores of other iron dithiolene tetramers are as follows: (1) A two-electron oxidation of the $[Fe_4(S_2C_2(CF_3)_2)_4(\mu_3\text{-}S)_4]^{2-}$ dianion to the neutral parent molecule would involve a removal of both electrons from a nondegenerate orbital which is highly antibonding among the four equivalent pairs of iron atoms; this would lead to a further relative shortening of the four Fe–Fe distances with maintenance of a tetragonal D_{2d} Fe_4S_4 geometry. For a one-electron oxidation of the dianion to the monoanion, one would expect either a similar D_{2d} Fe_4S_4 architecture with four shorter Fe–Fe bond lengths (based upon a loss of one electron from the above nondegenerate orbital) or alternatively an orthorhombic D_2 Fe_4S_4 configuration produced by a slight Jahn–Teller distortion arising from a removal of one electron from a doubly degenerate e orbital. (2) A replacement of the four terminal $S_2C_2(CF_3)_2$ ligands in the $[Fe_4(S_2C_2(CF_3)_2)_4(\mu_3\text{-}S)_4]^{2-}$ dianion with less π-acidic $S_2C_2(CN)_2$ ones would be expected to result in the frontier molecular orbitals possessing considerably larger antibonding Fe–Fe and Fe–S orbital character, which in turn should lead to significant increases in both the four short Fe–Fe and four vertical Fe–S bond lengths. The Fe_4S_4 cores of the corresponding neutral tetramers and monoanions of these two iron dithiolene series should also reflect similar Fe–Fe and Fe–S bond-length trends.

Further X-ray diffraction studies of these Fe_4S_4 clusters are needed as operational tests of these qualitative bonding predictions and as input data for quantitative MO calculations on these systems. Such stereochemical-bonding information is of prime relevance in a systematic assessment of the influence of different terminal ligands upon the structural and electronic parameters of cubanelike Fe_4S_4 systems.

Acknowledgment. This research was supported by the National Science Foundation. We are also grateful for an undergraduate fellowship to T.H.L. by Eastman Kodak Co.

Supplementary Material Available: A listing of the observed and calculated structure factors (21 pages). Ordering information is given on any current masthead page.

---

(35) (a) Trinh-Toan. Ph.D. Thesis, University of Wisconsin—Madison, 1972. (b) Teo, B.-K. Ph.D. Thesis, University of Wisconsin—Madison, 1973.

(36) The fact that Mössbauer spectra of the paramagnetic $[Fe_4(\eta^5\text{-}C_5H_5)_4(\mu_3\text{-}S)_4]^+$ monocation obtained in external fields (H_o) varying from 0 to 80 kOe at 4.2 K displayed no evidence for any magnetic hyperfine interaction at the iron sites resulted in the strong suggestion by Reiff and colleagues[34] that the unpaired electron in this monocation "does not interact with the iron sites and presumably occupies a predominantly ligand-based molecular orbital". This proposal appears to be incompatible with our qualitative metal cluster model as well as with the results of quantitative MO calculations[37] carried out with the Fenske–Hall program[38] on the entire $[Fe_4(\eta^5\text{-}C_5H_5)_4(\mu_3\text{-}S)_4]^n$ series and no other cubanelike M_4S_4 systems. In the absence of an applied magnetic field, the nonobservation of any magnetic hyperfine structure for the paramagnetic monocation at 4.2 K may be ascribed either to a lack of spin density at the iron sites or preferably from our viewpoint to the spin–lattice relaxation time being much shorter than the nuclear Larmor precession time such that the effective magnetic field at the iron nuclei (H_n) is time-averaged to 0.[39] The nondetection by Reiff and co-workers[34] of any hyperfine splitting in the magnetically perturbed Mössbauer spectra of the $[Fe_4(\eta^5\text{-}C_5H_5)_4(\mu_3\text{-}S)_4]^+$ monocation as the $[PF_6]^-$ salt may be due in part to its temperature-dependent magnetic moment[34] at 50–1.5 K being well below the spin-only value (e.g., 0.52 μ_B per mole of Fe at 4.2 K vs. 0.87 μ_B per mole of Fe); it is suggested[34] that these low magnitudes may reflect intercluster exchange interactions of negative sign.

(37) Campana, C. F. Ph.D. Thesis, University of Wisconsin—Madison, 1975. Campana, C. F.; Block, T. F.; Dahl, L. F., to be submitted for publication.

(38) Hall, M. B.; Fenske, R. F. *Inorg. Chem.* **1972**, *11*, 768–775.

(39) (a) Mössbauer, R. L.; Clauser, M. J. *Hyperfine Interact.* **1967**, 529–551. (b) Dekker, A. J. *Hyperfine Interact.* **1967**, 679–695. (c) Frankel, R. B.; Reiff, W. M.; Meyer, T. J.; Cramer, J. L. *Inorg. Chem.* **1974**, *13*, 2515–2517.

(40) (a) Dessy, R. E.; Reingold, A. L.; Howard, G. D. *J. Am. Chem. Soc.* **1972**, *94*, 746–752. (b) Dessy, R. E.; Bares, L. A. *Acc. Chem. Res.* **1972**, *5*, 415–421.

(41) Ginsburg, R. E.; Rothrock, R. K.; Finke, R. G.; Collman, J. P.; Dahl, L. F. *J. Am. Chem. Soc.* **1979**, *101*, 6550–6562.

(42) Teo, B. K.; Hall, M. B.; Fenske, R. F.; Dahl, L. F. *Inorg. Chem.* **1975**, *14*, 3103–3117.